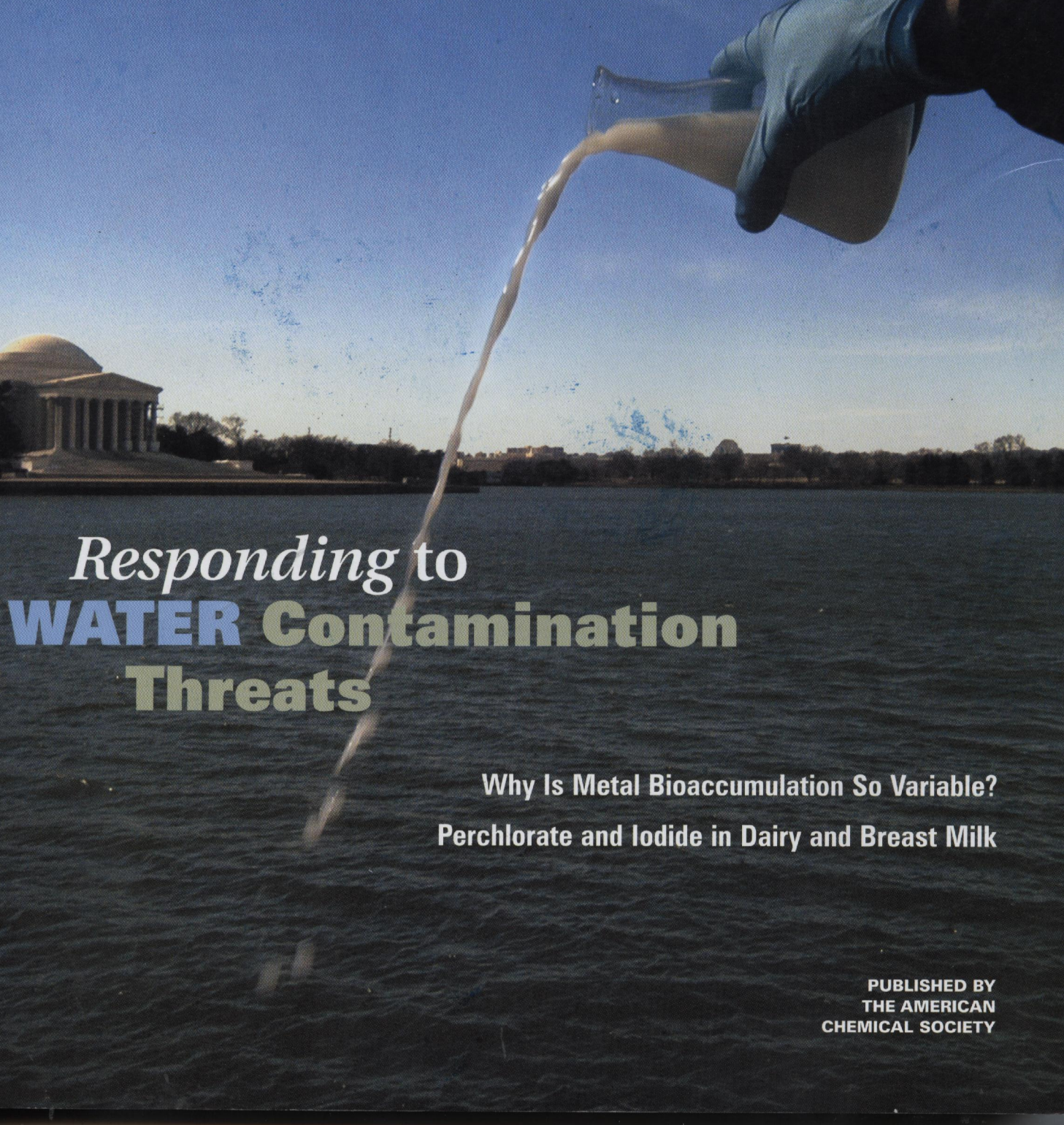


April 1, 2005

ENVIRONMENTAL Science & Technology

<http://pubs.acs.org/est>



Responding to **WATER Contamination** **Threats**

Why Is Metal Bioaccumulation So Variable?

Perchlorate and Iodide in Dairy and Breast Milk

PUBLISHED BY
THE AMERICAN
CHEMICAL SOCIETY

Research

Review

1921

Why Is Metal Bioaccumulation So Variable? Biodynamics as a Unifying Concept

Samuel N. Luoma and Philip S. Rainbow

Forecasts from biodynamic metal bioaccumulation models are tested against observations from nature and appear to explain variability among different species, metals, and environments.

Policy Analysis

■ 1932

Comparing Estimates of Persistence and Long-Range Transport Potential among Multimedia Models

Kathrin Fenner, Martin Scheringer, Matthew MacLeod, Michael Matthies, Thomas McKone, Maximilian Stroebé, Andreas Beyer, Mark Bonnell, Anne Christine Le Gall, Jörg Klasmeier, Donald Mackay, Dik van de Meent, David Pennington, Bernd Scharenberg, Noriyuki Suzuki, and Frank Wania

Overall persistence and long-range transport potential calculated with nine multimedia models are compared over a broad range of chemical properties.

1943

Comparative Advantage: The Impact of ISO 14001 Environmental Certification on Exports

Florencia Bellesi, David Lehrer, and Alon Tal

A survey among importers from six countries confirms the competitive advantage conferred by ISO 14001 certification in corporate acquisition decisions.

■ 1954

Quantification of Local and Global Benefits from Air Pollution Control in Mexico City

Galen McKinley, Miriam Zuk, Morten Höjer, Montserrat Avalos, Isabel González, Rodolfo Iniestra, Israel Laguna, Miguel A. Martínez, Patricia Osnaya, Luz M. Reynales, Raydel Valdés, and Julia Martínez

Costs, health benefits, and greenhouse gas emission reductions from air pollution control measures proposed for Mexico City are analyzed; policy implications are discussed.

Characterization of Natural and Affected Environments

1962

Characterization of Humic Substances by Environmental Scanning Electron Microscopy

Paul S. Redwood, Jamie R. Lead, Roy M. Harrison, Ian P. Jones, and Serge Stoll
Humic substances are visualized by environmental scanning electron microscopy and quantified by fractal dimensions as a function of solution conditions.

1967

Joint Sealants: An Overlooked Diffuse Source of Polychlorinated Biphenyls in Buildings

Martin Kohler, Josef Tremp, Markus Zennegg, Cornelia Seiler, Salome Minder-Kohler, Marcel Beck, Peter Lienemann, Lukas Wegmann, and Peter Schmid
Joint sealants in buildings erected between 1955 and 1975 represent a significant inventory of PCBs and may lead to elevated PCB indoor air concentrations.

1974

Microbial Catabolic Diversity in Soils Contaminated with Hydrocarbons and Heavy Metals

Wei Shi, Marianne Bischoff, Ronald Turco, and Allan Konopka

Highly contaminated soils are capable of using a broad spectrum of organic substrates.

1980

Occupational Exposure to Commercial Decabromodiphenyl Ether in Workers Manufacturing or Handling Flame-Retarded Rubber

Kaj Thuresson, Åke Bergman, and Kristina Jakobsson

Workers manufacturing or handling decaBDE flame-retarded rubber show up to 270 ng/g lipid weight of decaBDE (BDE-209) in their serum.

1987

► Hexabromocyclododecane in Marine Species from the Western Scheldt Estuary: Diastereoisomer- and Enantiomer-Specific Accumulation

Karel Janák, Adrian Covaci, Stefan Voorspoels, and Georg Becher

Hexabromocyclododecane diastereomers and their enantiomer fractions are determined in marine biota of the Western Scheldt estuary by reversed-phase and chiral chromatography with mass spectrometric detection.

■ 1995

Polychlorinated Dioxins and Furans from the World Trade Center Attacks in Exterior Window Films from Lower Manhattan in New York City

Sierra Rayne, Michael G. Ikonomou, Craig M. Butt, Miriam L. Diamond, and Jennifer Truong

Concentrations and patterns of polychlorinated dibenzo-*p*-dioxins and furans are observed in exterior window films from Lower Manhattan after the World Trade Center attacks.

2004

Climate Dependency of Tree Growth Suppressed by Acid Deposition Effects on Soils in Northwest Russia

Gregory B. Lawrence, Andrei G. Lapenit, Dan Berggren, Boris F. Aparin, Kevin T. Smith, Walter C. Shortle, Scott W. Bailey, Dmitry L. Varlyguin, and Boris Babikov

Calcium depletion and aluminum mobilization, attributable to acid deposition, are found to coincide with pronounced growth declines and suppression of climate responses of Norway spruce.

2011

► Perchlorate and Iodide in Dairy and Breast Milk

Andrea B. Kirk, P. Kalyani Martinelango, Kang Tian, Aniruddha Dutta, Ernest E. Smith, and Purnendu K. Dasgupta

Perchlorate is a common contaminant of human and cow milk and at higher levels is correlated with low iodide content of breast milk.

2018

Lead Isotopic Composition of Fly Ash and Flue Gas Residues from Municipal Solid Waste Combustors in France: Implications for Atmospheric Lead Source Tracing

Jean Carignan, Guy Libourel, Christophe Cloquet, and Lydie Le Forestier

This study suggests that the lead isotopic composition of municipal solid waste combustor materials represents the average composition of industrial lead emitted to the atmosphere.

Environmental Processes

2025

Adsorption of 4-Picoline and Piperidine to the Hydrated SiO₂ Surface: Probing the Surface Acidity with Vibrational Sum Frequency Generation Spectroscopy

Dingfang Liu, Gang Ma, and Heather C. Allen

The adsorption of 4-picoline onto a silica surface occurs through weak hydrogen bonds, and piperidine adsorption occurs through protonation.

■ 2033

Characterization of Aromatic Compound Sorptive Interactions with Black Carbon (Charcoal) Assisted by Graphite as a Model

Dongqiang Zhu and Joseph J. Pignatello

Isotherms of substituted benzenes normalized for hydrophobic effects combined with spectroscopic data on solution-phase model systems reveal size-exclusion effects and surface π-π electron donor-acceptor interactions.

► Supporting information is available free at <http://pubs.acs.org/est>.

► This issue contains a news story about this research.

2042

Ligand Arsenic Complexation and Immunoperoxidase Detection of Metallothionein in the Earthworm *Lumbricus rubellus* Inhabiting Arsenic-Rich Soil

C. J. Langdon, C. Winters, S. R. Stürzenbaum, A. J. Morgan, J. M. Charnock, A. A. Meharg, T. G. Pearce, P. H. Lee, and K. T. Semple

X-ray absorption spectrometry and immunoperoxidase histochemistry in selected tissues of earthworms detect arsenic in the form of thiol groups, which suggests the presence of As::metallothionein.

2049

Confocal Micrometer-Scale X-ray Fluorescence and X-ray Absorption Fine Structure Studies of Uranium Speciation in a Tertiary Sediment from a Waste Disposal Natural Analogue Site

Melissa A. Denecke, Koen Janssens, Kristof Proost, Jörg Rothe, and Ulrich Noseck

μ -XRF and μ -XAFS measurements in confocal geometry of a uranium-rich sediment show uranium to be a tetravalent phosphate and associated with mixed-valent arsenic.

2059

Reoxidation of Reduced Uranium with Iron(III) (Hydr)Oxides under Sulfate-Reducing Conditions

Rajesh K. Sani, Brent M. Peyton, Alice Dohnalkova, and James E. Amonette

Biological reduction and reoxidation of uranium under lactate-limited sulfate-reducing conditions in the presence of iron(III) (hydr)oxides are presented.

2067

Toward a Biotic Ligand Model for Freshwater Green Algae: Surface-Bound and Internal Copper Are Better Predictors of Toxicity than Free Cu²⁺-Ion Activity When pH Is Varied

Karel A. C. De Schampelaere, Jennifer L. Stauber, Karyn L. Wilde, Scott J. Markich, Paul L. Brown, Natasha M. Franklin, Nicola M. Creighton, and Colin R. Janssen

When pH is varied, surface-bound and internal coppers are better predictors of copper toxicity to unicellular green microalgae than Cu²⁺ ion activity.

2073

Oxidation of Nanomolar Levels of Fe(II) with Oxygen in Natural Waters

J. Magdalena Santana-Casiano, Melchor González-Dávila, and Frank J. Millero

A model predicts the oxidation rate of Fe(II) by molecular oxygen at nanomolar levels valid in seawater with different pH, salinity, and temperature.

2080

Root-Induced Cycling of Lead in Salt Marsh Sediments

Bjorn Sundby, Miguel Caetano, Carlos Vale, Charles Gobeil, George W. Luther, III, and Donald B. Nuzzio

Lead solubility and lead cycling between salt marsh sediments and plants are linked to the annual growth and decay cycle of roots.

2087

Catalysis of Elemental Sulfur Nanoparticles on Chromium(VI) Reduction by Sulfide under Anaerobic Conditions

Yeqing Lan, Baolin Deng, Chulsung Kim, Edward C. Thornton, and Huifang Xu

The reaction between chromate and hydrogen sulfide produces elemental sulfur nanoparticles as product, which catalyzes further chromate reduction.

2095

► Levels of Hexabromocyclododecane in Harbor Porpoises and Common Dolphins from Western European Seas, with Evidence for Stereoisomer-Specific Biotransformation by Cytochrome P450

Bart N. Zegers, Anchelique Mets, Ronald van Bommel, Chris Minkenberg, Timo Hamers, Jorke H. Kamstra, Graham J. Pierce, and Jan P. Boon

Biotransformation by the cytochrome P450 system is the most likely process to explain the exclusive accumulation of Σ -HBCD in harbor porpoises and common dolphins.

2101

UV Photolytic Mechanism of *N*-Nitrosodimethylamine in Water: Dual Pathways to Methylamine versus Dimethylamine

Changha Lee, Wonyong Choi, Young Gyu Kim, and Jeayong Yoon

This study reveals a new mechanistic pathway of NDMA photolysis to DMA by identifying the factors influencing the photolysis pathway.

2107

Pu(V) O_2^+ Adsorption and Reduction by Synthetic Hematite and Goethite

Brian A. Powell, Robert A. Fjeld, Daniel I. Kaplan, John T. Coates, and Steven M. Serkiz

Pu(V) adsorption and reduction on synthetic hematite and goethite is examined, demonstrating a pathway for plutonium retardation during subsurface transport.

2115

Isomer-Selective Adsorption of Amino Acids by Components of Natural Sediments

M. Wedyan and M. R. Preston

Treated natural sediments and three component minerals (quartz, kaolin, and montmorillonite) show selective adsorptive behavior between the D and L isomers of amino acids.

2120

Methyl Arsenic Adsorption and Desorption Behavior on Iron Oxides

B. J. Lafferty and R. H. Loepert

The adsorption and desorption of mono- and dimethyl arsenic(III) and arsenic(V) on iron oxide minerals are evaluated with adsorption isotherms, adsorption envelopes, and desorption envelopes.

2128

Mechanisms of Dioxin Formation from the High-Temperature Oxidation of 2-Bromophenol

Catherine S. Evans and Barry Dellinger

The formation of PBDD/F and PCDD/F from halogenated phenols is compared for oxidative, postflame, and combustion conditions.

2135

Uptake, Metabolism, Accumulation, and Toxicity of Cyanide in Willow Trees

Morten Larsen, Ahmed S. Ucisik, and Stefan Trapp

The relationship among uptake, metabolism, accumulation, and toxicity of cyanide in willow trees is simulated with a nonlinear mathematical model and validated with experimental results.

2143

Time-Dependent Sorption-Desorption Behavior of 2,4-Dichlorophenol and Its Polymerization Products in Surface Soils

Mónica Palomo and Alok Bhandari

Solute extractability data suggest that sorption of 2,4-dichlorophenol and its polymerization products continued long after apparent sorption equilibrium.

2152

XANES Investigation of Phosphate Sorption in Single and Binary Systems of Iron and Aluminum Oxide Minerals

Nidhi Khare, Dean Hesterberg, and James D. Martin

Phosphorus K-XANES analysis shows that phosphate sorption mechanisms in iron- and aluminum-oxide mixtures are not always the same as in single-mineral systems.

2161

Determination of Stability Constants of U(VI)-Fe(III)-Citrate Complexes

Cetin Kantar, Jeff B. Gillow, Ruth Harper-Arabie, Bruce D. Honeyman, and Arokiasamy J. Francis

The formation of 1:1:1 and 1:1:2 Fe(III)-U(VI)-citrate complexes must be included in U(VI) speciation calculations when Fe(III) is present.

2169

Thermodynamic Analysis of Arsenic Methylation

Paul M. Dombrowski, Wei Long, Kevin J. Farley, John D. Mahony, Joseph F. Capitani, and Dominic M. Di Toro

Equilibrium chemistry is used to investigate the thermodynamics of arsenic methylation with formation energies estimated by quantum chemical methods.

Environmental Modeling

2177

Spatial Variability and Uncertainty in Ecological Risk Assessment: A Case Study on the Potential Risk of Cadmium for the Little Owl in a Dutch River Flood Plain

Lammert Kooistra, Mark A. J. Huijbregts, Ad M. J. Ragas, Ron Wehrens, and Rob S. E. W. Leuven

A new methodology is presented that compares different sources of spatial variability and uncertainty in ecological risk assessment.

2188

Practical Considerations on the Use of Predictive Models for Regulatory Purposes

Jay Tunkel, Kelly Mayo, Carlye Austin, Amy Hickerson, and Philip Howard

Practical issues are explored to study the regulatory applicability and predictive power of rat oral lethality and fish acute toxicity QSAR models.

■ 2200

Identification of Temperature-Dependent Water Quality Changes during a Deep Well Injection Experiment in a Pyritic Aquifer

Henning Prommer and Pieter J. Stuyfzand

Three-dimensional geochemical transport modeling is used to identify and quantify temperature-dependent water quality changes during a deep-well injection experiment in a pyritic aquifer.

Environmental Measurements Methods

■ 2210

Application of Quantitative Fluorescence and Absorption-Edge Computed Microtomography to Image Metal Compartmentalization in *Alyssum murale*

David H. McNear, Jr., Edward Peltier, Jeff Everhart, Rufus L. Chaney, Steve Sutton, Matt Newville, Mark Rivers, and Donald L. Sparks

Computed microtomographic techniques can be used to accurately determine the concentration and compartmentalization of metals within hyperaccumulating plant tissue.

2219

Adaptation of Dry Nephelometer Measurements to Ambient Conditions at the Jungfraujoch

Remo Nessler, Ernest Weingartner, and Urs Baltensperger

A method is presented to adapt dry nephelometer measurements to ambient conditions without the need for additional data except ambient relative humidity.

2229

Comparison of Mass-Based and Non-Mass-Based Particle Measurement Systems for Ultra-Low Emissions from Automotive Sources

Martin Mohr, Urs Lehmann, and Josef Rütter

Different particle mass measurement systems are compared on a heavy-duty diesel engine to investigate their feasibility for particle characterization for future ultralow concentration levels.

2239

Nond derivatization Analytical Method of Fatty Acids and *cis*-Pinonic Acid and Its Application in Ambient PM_{2.5} Aerosols in the Greater Vancouver Area in Canada

Yu Cheng and Shao-Meng Li

A non derivatization method is developed to analyze C₆–C₂₀ fatty acids and *cis*-pinonic acid on GC/FID and GC/MSD using a polar DB-FFAP capillary column.

2247

Novel Algorithm for Tomographic Reconstruction of Atmospheric Chemicals with Sparse Sampling

Wim Verkrusse and Lori A. Todd

A novel image-reconstruction method may allow scientists to create 2-D and 3-D chemical concentration maps that visualize the flow of contaminants in air.

2255

Differential Pressure as a Measure of Particulate Matter Emissions from Diesel Engines

Steven E. Mischler and Jon C. Volkwein

Samples from different diesel engines running under various RPM and load scenarios are collected, analyzed, and compared to elemental carbon concentrations in the sampled exhaust.

2262

Convenient New Chemical Actinometer Based on Aqueous Acetone, 2-Propanol, and Carbon Tetrachloride

Heng Li, Eric A. Betterton, Robert G. Arnold, Wendell P. Ela, Brian Barbaris, and Cecilio Grachane

A new chemical actinometer conveniently measures ultraviolet solar irradiance and spectral outputs from laboratory light sources without light-sensitive compounds, difficult analyses, or prolonged exposures.

Remediation and Control Technologies

2267

Optimizing Contaminant Desorption and Bioavailability in Dense Slurry Systems. 1. Rheology, Mechanical Mixing, and PAH Desorption

Walter J. Weber, Jr., and Han S. Kim

These slurries act like pseudoplastic non-Newtonian fluids, and the impeller revolution rate and its diameter have dramatic impacts on power and torque requirements.

2274

Optimizing Contaminant Desorption and Bioavailability in Dense Slurry Systems. 2. PAH Bioavailability and Rates of Degradation

Han S. Kim and Walter J. Weber, Jr.

Rates of phenanthrene biodegradation are markedly enhanced by relatively low level auger mixings under both aerobic and anaerobic (denitrifying) conditions.

2280

Reductive Debromination of Polybrominated Diphenyl Ethers by Zerovalent Iron

Young-Soo Keum and Qing X. Li

Bromodiphenyl ethers are debrominated by iron and sulfides, which can be a means of remediation and may be a mechanism for their degradation in the environment.

2287

Fate of Wastewater Effluent hER-Agonists and hER-Antagonists during Soil Aquifer Treatment

Otakuye Conroy, David M. Quanrud, Wendell P. Ela, Daniel Wicke, Kevin E. Lansey, and Robert G. Arnold

Application of a modified reporter-gene assay shows that estrogenic and anti-estrogenic compounds can be present simultaneously in complex environmental waste samples.

2294

Accelerated Transformation and Deactivation of Erythromycin in Superheated Water. 1. Temperature Effects, Transformation Rates, and the Impacts of Dissolved Organic Matter

Michelle N. Butler and Walter J. Weber, Jr.

Accelerated conversion of erythromycin occurs in water under superheated conditions, with >85% conversion in 30 min at temperatures of 125–200 °C.

2301

Accelerated Transformation and Deactivation of Erythromycin in Superheated Water. 2. Transformation Reactions and Bioassays

Michelle N. Butler and Walter J. Weber, Jr.

Analyses of reactor effluents indicate that the initial step in the decomposition pathway is one of dehydration followed by subsequent hydrolysis.

■ Supporting information is available free at <http://pubs.acs.org/est>.

► This issue contains a news story about this research.